3986–3995 *Nucleic Acids Research, 2019, Vol. 47, No. 8* *Published online 30 January 2019*
doi: 10.1093/nar/gkz048

The absence of the catalytic domains of *Saccharomyces cerevisiae* DNA polymerase ε strongly reduces DNA replication fidelity

Marta A. Garbacz[1], Phillip B. Cox[1], Sushma Sharma[2], Scott A. Lujan[1], Andrei Chabes[2] and Thomas A. Kunkel[1,*]

[1]Genome Integrity and Structural Biology Laboratory, National Institute of Environmental Health Sciences, NIH, DHHS, Research Triangle Park, NC 27709, USA and [2]Medical Biochemistry and Biophysics, Umeå University, SE-901 87 Umeå, Sweden

Received October 31, 2018; Revised January 15, 2019; Editorial Decision January 16, 2019; Accepted January 23, 2019

ABSTRACT

The four B-family DNA polymerases α, δ, ε and ζ cooperate to accurately replicate the eukaryotic nuclear genome. Here, we report that a *Saccharomyces cerevisiae* strain encoding the *pol2-16* mutation that lacks Pol ε's polymerase and exonuclease activities has increased dNTP concentrations and an increased mutation rate at the *CAN1* locus compared to wild type yeast. About half of this mutagenesis disappears upon deleting the *REV3* gene encoding the catalytic subunit of Pol ζ. The remaining, still strong, mutator phenotype is synergistically elevated in an *msh6Δ* strain and has a mutation spectrum characteristic of mistakes made by Pol δ. The results support a model wherein slow-moving replication forks caused by the lack of Pol ε's catalytic domains result in greater involvement of mutagenic DNA synthesis by Pol ζ as well as diminished proofreading by Pol δ during replication.

INTRODUCTION

Eukaryotic nuclear DNA replication is largely conducted by the four B-family DNA polymerases (Pols), Pols α, δ, ε and ζ. Pol α initiates replication by synthesizing short RNA-DNA primers that are then used by Pols δ and ε to synthesize the majority of the lagging and leading DNA strands, respectively (1–4). The fourth B-family member, Pol ζ, is more specialized and contributes to DNA synthesis when more difficult-to-replicate sequences are encountered (5,6). Pols α and ζ lack intrinsic exonuclease activity, while Pols δ and ε have 3′-exonucleases that can proofread mismatches. Pols α and ζ lack intrinsic exonuclease activity, such that the accuracy with which they synthesize DNA depends primarily on their nucleotide selectivity. Pols δ and ε have high nucleotide selectivity and they also have 3′-exonucleases that can proofread mismatches to further improve accuracy. Thus, Pols ε and δ synthesize DNA with very high fidelity, with average base substitution error rates of $<2.0 \times 10^{-5}$ for Pol ε and less than 1.3×10^{-5} for Pol δ, and average single nucleotide deletions error rates of less than 5.0×10^{-7} for Pol ε and $<1.3 \times 10^{-5}$ for Pol δ (7,8). Thus, the high fidelity of nuclear DNA replication in unstressed eukaryotic cells is thought to reflect the ability of these four DNA polymerases to select and incorporate correct nucleotides, proofreading by Pols δ and ε during replication, and DNA mismatch repair (MMR) that corrects mismatches that escape proofreading (9–11).

This general understanding of how replication fidelity is achieved has been supported by many studies (see below), including those that attempt to more precisely understand where and when each of the four B-family DNA polymerases functions during replication of large and complex eukaryotic genomes (1). Studies published in the last few years suggest two different models for replication of the unstressed nuclear genome, one in which Pol δ is the major replicase for both DNA strands (12) and the other proposing that Pol ε has a major role in leading strand replication (2,13–21). The latter model is supported by a study published earlier this year of the yeast *pol2-16* mutant (22), which lacks the catalytic domains for polymerization and proofreading by Pol ε. This strain survives by replicating the nuclear genome using Pol δ as the primary replicase for both the leading and lagging DNA strands. However, cell growth in the *pol2-16* mutant is aberrant, as indicated by elongated S-phase an increased doubling time, larger than normal cells that contain aberrant nuclei, and rapid acquisition of suppressors. In the present study, we add another endpoint, a mutator phenotype indicating that replication fidelity is strongly reduced when the catalytic domains of

*To whom correspondence should be addressed. Tel: +1 984 287 4281; Fax: +1 919 541 7613; Email: kunkel@niehs.nih.gov

Pol ε are missing. The new data suggest that this mutator effect is partly due to reduced proofreading by Pol δ and partly due to errors generated by Pol ζ.

MATERIALS AND METHODS

Yeast strains construction

Saccharomyces cerevisiae strains used in this study are listed in Supplemental Materials. All yeast strains were isogenic derivatives of AC402 and AC403, representing the W303 background. Wild type diploids of W303 background and the *pol2-16* mutants were generated as described earlier (22). Strains bearing the *pol3L612M* polymerase variant were constructed via an integration-excision method using plasmid p170-pol3L612M (23). Strains with deletion of *REV3 (rev3Δ)* and *MSH6* (*msh6Δ)* were constructed using one-step gene disruption as follows. PCR product containing the *rev3Δ::KanMX4* cassette was amplified from genomic DNA of YPL167C using as primers 5_REV3_F and 3_REV3_R. The presence of the *rev3Δ::KanMX4* in transformants that were G-418^r was confirmed by PCR using primers up_REV3_f and pTEF. PCR product containing *msh6Δ::Kl-LEU2* - cassette was amplified from pUG73 using primers MSH6-LEU2-5 and MSH6-LEU2-3′. The presence of *msh6Δ::Kl-LEU2* in transformants that were LEU2$^+$ was confirmed by PCR using primers up_msh6_5′_f and Kl-LEU2_5′_r. Primer sequences are provided in the Supplementary Data 1.

Mutation rate measurements

To determine spontaneous mutation rates, at least 24 independent cultures of each yeast strain (two independent isolates) were inoculated with a single yeast colony or a spore colony in 5 ml of liquid YPDA supplemented with adenine to a final concentration of 100 mg/l. Cultures were grown at 23°C to the stationary phase (for 5 days in case of the *pol2-16* mutant or 3 days for *POL2*) and plated on selective and nonselective media. Plates were incubated at 23°C for 8 days and colonies were scored. The mean mutation rates as well as 95% confidence intervals were calculated as described in (24). To determine *P*-values for significance of differences of the mutation rates between strains the Mann–Whitney U non-parametric test and GraphPad Prism 7 software was used.

CAN1 mutation spectra analysis

The Can^r colonies for mutational spectrum analysis at the *CAN1* locus were collected as described previously (25). Primers Can1-AF and Can1-BR were used for *CAN1* locus amplification and primers Can1_BR, Can1_AR, Can1_9R and Can1_10R were used for sequencing. Sequences of all oligonucleotides are listed in the Supplementary Data 1. Mutations in *CAN1* were called using SeqMan DNASTAR Navigator sequence assembly software. Graphical representation of analyzed mutation spectra are presented in Supplementary Data 2. Statistical significance of differences between two spectra were determined using a Monte Carlo method as described in (24,26). Likewise for determining the significance of differences between ratios of reciprocal mutation rate between two data sets, i.e. a ratio of ratios. Significance cutoffs were selected with Šidák correction for multiple hypothesis testing based on a familywise error rate of 5% (27).

dNTP pools measurement

dNTP pools were measured in three independent spore colonies of each genotype, from a freshly dissected heterozygous diploid *pol2-16/POL2*. Cells were inoculated in YPD medium supplemented with 100 mg/l adenine and grown at 23°C to OD_{600} between 0.35 and 0.4. Cells equivalent to 30 OD units were harvested by filtration, immediately suspended in an ice-cold trichloroacetic acid-$MgCl_2$ mixture, flash frozen in liquid nitrogen. Samples were further proceeded as described previously (28).

Flow cytometry

Cells from an asynchronously growing culture were processed and analyzed for cell cycle progression by Becton Dickinson FC500 flow cytometer as described previously (29).

Immunoblotting for Sml1 expression

5 OD units of yeast cells collected at log phase (OD_{600} between 0.3 and 0.7) were resuspended in TCA buffer (20 mM Tris, pH 8, 50 mM ammonium acetate, 2 mM EDTA) supplemented with protease inhibitors (cOmplete EDTA-free protease inhibitors, Roche) and vortexed with glass beads at 4°C. Sml1 was detected using anti-Sml1 antibody (AS10 847, Agrisera) at 1:1000 dilution. Pstair was used as loading control, and detected with an antibody against pstair (Sigma, P7962) at 1:5000 dilution. Western Blots were developed using chemiluminescent substrates for HRP (WesternBright Sirius, advansta), and images were taken using G:BOX (SYNGENE).

RESULTS

Aberrant cell cycle progression, S-phase checkpoint activation and increased dNTP pools in *pol2-16*

Because the *pol2-16* mutant quickly accumulates suppressors (22), here and throughout this study we use freshly isolated haploid *pol2-16* colonies obtained from spores germinated from meiotic progeny of heterozygous diploid *pol2-16/POL2* strains. Compared to wild type colonies, three independent *pol2-16* mutant colonies exhibited aberrant progression through the cell cycle when analyzed by flow cytometry (Figure 1A). These results are consistent with our earlier study (22) demonstrating that, as compared to wild type, *pol2-16* mutant cells are larger, grow more slowly and have aberrant nuclei (22). Moreover, *pol2-16* cells also have dNTP concentrations that are elevated from 3-fold (for dGTP) to 5.5-fold (for dCTP) (Figure 1B). Consistent with such stress-related phenotypes, the *pol2-16* mutant also has an activated S-phase checkpoint. The level of Sml1, an indicator of S-phase checkpoint activation, is significantly decreased to the level observed in wild type yeast treated with 4-NQO (Figure 1C).

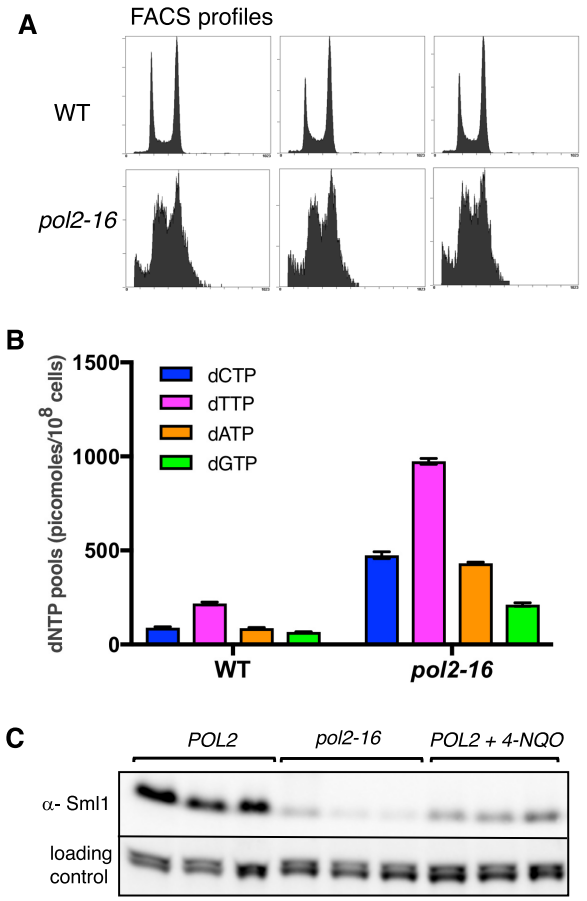

Figure 1. Lack of Pol ε catalytic domains (*pol2-16*) leads to replication stress. (**A**) Flow cytometry profiles of log phase yeast cultures of wild type and *pol2-16* strains used for dNTP pool measurements; (**B**) intracellular dNTP levels; presented as mean values ± SD ($n = 3$); (**C**) western blot detection of Sml1 levels in whole cell extracts of the wild type, *pol2-16* and wild type strains treated with the 4-nitroquinoline 1-oxide (4-NQO) at 0.2 μg/ml for 4 h, representative of two independent measurements is presented.

An increased mutation rate in *pol2-16* mutant

Next we measured the spontaneous mutation rates in the *pol2-16* and wild type strains using the *CAN1* reporter gene. Compared to a mutation rate of 4.1×10^{-7} in wild type cells, the *pol2-16* mutant has mutation rate of 110×10^{-7} (Table 1). This 27-fold increase is substantial ($P < 0.0001$, Supplementary Data 1), being six times larger than that observed in a *pol2-4* strain that lacks Pol ε proofreading and about three times larger than the rate in an *msh6Δ* strain that is partially defective in MMR of replication errors (Table 1). To understand the source of the mutations that spontaneously occur in the *pol2-16* mutant, we sequenced Can^r colonies (Table 2 and Supplementary Table S1), calculated mutation rates for various substitutions and insertions/deletions (indels) (Table 2 and Supplementary Table S1), and then compared the rates in wild type yeast (Figure 2A) to those in the *pol2-16* mutant (Figure 2C). The mutation rates are increased in the *pol2-16* mutant by factors ranging from about 10- to 130-fold (Figure 2E, Table 2 and Supplementary Table S1).

Table 1. Spontaneous mutation rates in the *pol2-16*, *rev3Δ*, *msh6Δ*, *pol3L612M* mutant alone and in combinations

Strain	Mutation Rate [Can^r x 10^{-7}]	Relative rate (mutants vs. *wt*)
Wild type	4.1[a] (3.7–4.4) [b]	1.0[c]
pol2-16	110 (96–120)	26.8
pol2-4	18.0 [d]	4.4
msh6Δ	40 (35–46)	9.8
pol2-16 msh6Δ	570 (450–730)	139.0
rev3Δ	2.4 (2.1–2.6)	0.6
pol2-16 rev3Δ	50 (42–59)	12.2
rev3Δ msh6Δ	49 (43–57)	12.0
pol2-16 rev3Δ msh6Δ	320 (260–410)	78.1
pol3L612M	29 (22–37)	7.1
pol2-16 pol3L612M	670 (490–910)	163.4

[a]Mean value of the mutation rates are presented as Can^r x 10^{-7};
[b]95% CL range of mutation rates are presented in parentheses;
[c]Relative rate is the mutation rate in a given strain divided by the mutation rate in the wild type strain;
[d]Mutation rate taken from (25).

Partial suppression of *pol2-16* mutator effect by deletion of *REV3*

The results in Figure 2C suggest that the loss of Pol ε catalytic activities in the *pol2-16* mutant may promote two different sets of replication errors. One set includes A•T to G•C, G•C to A•T and G•C to T•A substitutions and single-base deletion mutations (colored green in Figure 2). This is interesting because, although there are many types of base-base substitution and indel mismatches that theoretically can be made during DNA replication, it is these specific mutations that are preferentially made by Pol δ, through T•dGMP, G•dTMP, C•dTMP and single-base deletion mistakes (30). Moreover, Pol δ is the polymerase implicated by HydEn-seq analysis of ribonucleotide incorporation to perform the bulk of replication of both DNA strands in the *pol2-16* mutant (22).

The second set of errors in the *pol2-16* mutant are A•T to C•G, A•T to T•A and G•C to C•G transversions and complex errors involving multiple clustered changes (all colored pink in Figure 2C). This second set of errors has previously been observed to disappear in yeast strains defective in Pol ζ (*rev3Δ*) (31–35), suggesting that these errors may be generated by Pol ζ. We therefore deleted the *REV3* gene encoding the catalytic subunit of Pol ζ and then compared the mutation rate and specificity in the double mutant *pol2-16 rev3Δ* strain to that in the single mutants. Consistent with a role for Pol ζ in spontaneous mutagenesis, and as expected based on previous results (25,31–33,36–38) (and see discussion below), the *rev3Δ* strain has an approximately 2-fold lower mutation rate than the wild type yeast (Table 1 and Figure 2B; $P < 0.0001$, Supplementary Table S1). Importantly for the present study, this is also the case for the *pol2-16* mutant, where the mutation rate dropped from 110×10^{-7} in *pol2-16* to 50×10^{-7} in the *pol2-16 rev3Δ* double mutant (Table 1; $P < 0.0001$, Supplementary Data 1). Moreover, the analysis of mutational specificity reveals that in the *pol2-16 rev3Δ* double mutant strain, the rates for the second set of mutations (pink in Figure 2C and D) are diminished by 88-, 13- and 8- fold, respectively, for G•C to C•G, A•T to T•A,

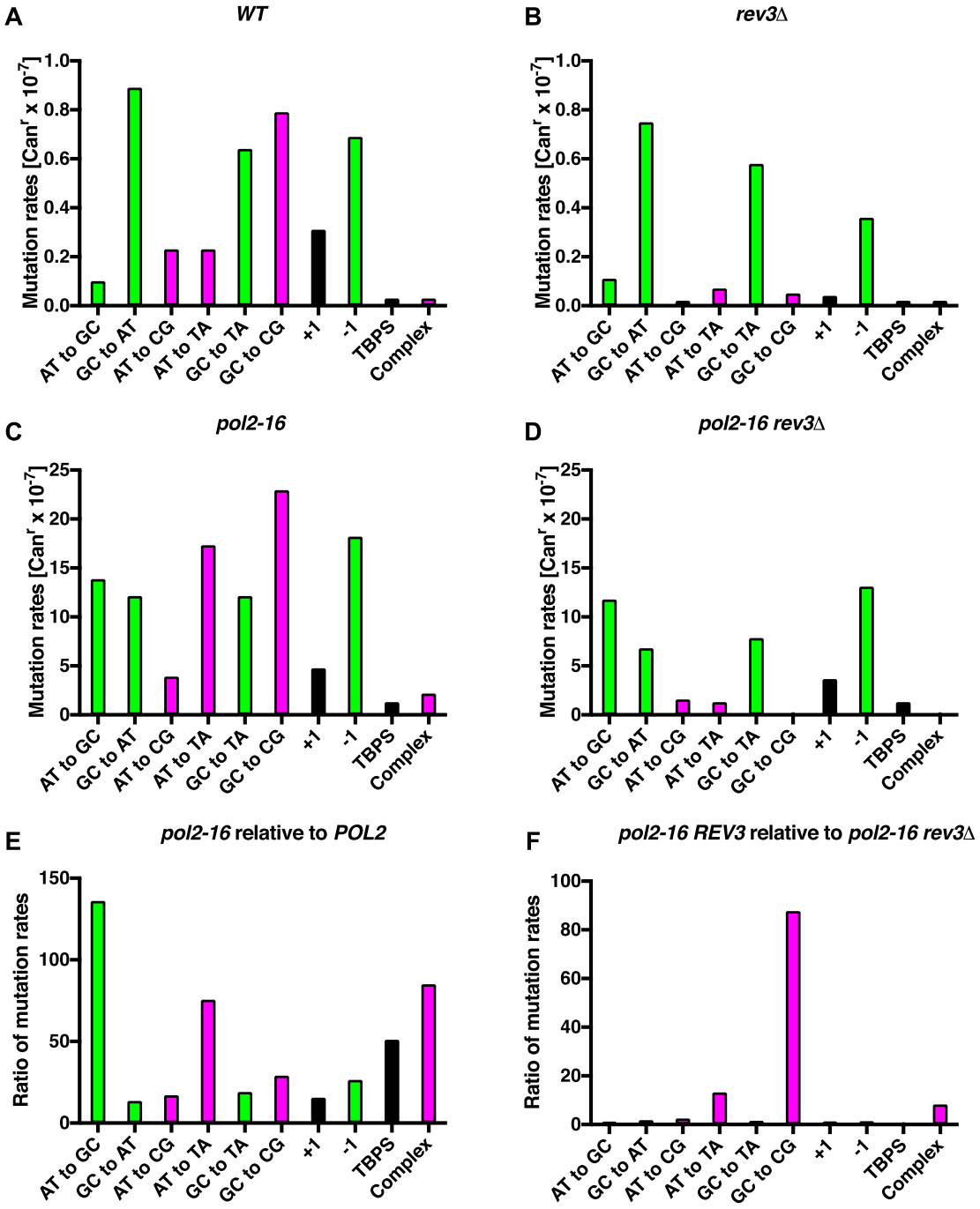

Figure 2. Pol ζ is responsible for a fraction of mutations in the *pol2-16* mutant. Diagrams **A**–**D** show the mutation rates of specific mutation classes measured for wild type, *pol2-16*, *rev3Δ* and *pol2-16 rev3Δ* yeast. Data in panels A–D are from Table 2. Panels **E** and **F** present ratios of mutation rates of specific mutation classes. Pink bars indicate mutation types characteristic for Pol ζ, green bars indicate mutation types characteristic for Pol δ (see text). Black bars represent other mutations (not Pol δ or ζ-dependent). TBPS are tandem base pair substitutions.

and complex mutations (Figure 2F; for all three mutation types $P \leq 0.0001$, Supplementary Data 1), while the first set of mutations that includes A•T to G•C, G•C to A•T, G•C to T•A and one nucleotide deletions (in green) is only marginally affected by the *rev3Δ*, being decreased by 1.2-, 1.8-, 1.5- and 1.4-fold, respectively (for all four mutation types, p is >0.00029, the Šidák cutoff for a familywise error rate of 0.05).

Suppression of *pol2-16 rev3Δ* mutator effect by mismatch repair

To determine whether the mutator effects in the *pol2-16 rev3Δ* strain depend on Pol δ, we performed two types of

Table 2. Mutation rates of specific mutation types detected in Can^r yeast colonies

Type of mutation/ Strain	WT	*pol2-16*	*rev3Δ*	*pol2-16 rev3Δ*	*pol2-16 rev3Δ msh6Δ*	*pol2-16 pol3L612M*	*pol3L612M*
Base substitutions	2.88 [a] (113) [b]	82.28 (190)	1.58 (87)	29.58 (113)	285.22 (164)	368.66 (115)	18.7 (118)
Transitions	0.99 (39)	25.98 (60)	0.85 (47)	18.59 (71)	205.22 (118)	182.73 (57)	12.68 (80)
AT→GC	0.1 (4)	13.86 (32)	0.11 (6)	11.78 (45)	76.52 (44)	57.7 (18)	5.55 (35)
GC→AT	0.89 (35)	12.13 (28)	0.75 (41)	6.81 (26)	128.7 (74)	125.02 (39)	7.13 (45)
Transversions	1.88 (74)	56.3 (130)	0.73 (40)	10.99 (42)	80 (46)	185.93 (58)	6.02 (38)
AT→CG	0.23 (9)	3.9 (9)	0.02 (1)	1.57 (6)	3.48 (2)	32.06 (10)	1.9 (12)
AT→TA	0.23 (9)	17.32 (40)	0.07 (4)	1.31 (5)	1.74 (1)	32.06 (10)	1.27 (8)
GC→TA	0.64 (25)	12.13 (28)	0.58 (32)	7.85 (30)	74.78 (43)	102.58 (32)	2.22 (14)
GC→CG	0.79 (31)	22.95 (53)	0.05 (3)	0.26 (1)	<1.74 (<1)	19.23 (6)	0.63 (4)
InDels [c]	0.99 (39)	22.95 (53)	0.4 (22)	16.75 (64)	31.3 (18)	298.13 (93)	9.83 (62)
+ 1	0.31 (12)	4.76 (11)	0.04 (2)	3.66 (14)	12.17 (7)	48.09 (15)	1.27 (8)
− 1	0.69 (27)	18.19 (42)	0.36 (20)	13.09 (50)	19.13 (11)	250.05 (78)	8.56 (54)
Insertions ≥2	0.08 (3)	0.43 (1)	0.07 (4)	0.79 (3)	1.74 (1)	<3.21 (<1)	0.16 (1)
Deletions ≥2	0.15 (6)	0.87 (2)	0.35 (19)	1.57 (6)	1.74 (1)	<3.21 (<1)	0.16 (1)
TBPS [d]	<0.03 (<1)	1.3 (3)	0.02 (<1)	1.31 (5)	<1.74 (<1)	<3.21 (<1)	0.16 (1)
Complex [e]	<0.03 (<1)	2.17 (5)	<0.02 (<1)	<0.26 (<1)	<1.74 (<1)	3.21 (1)	<0.16 (<1)
Total	4.1 (161)	110 (254)	2.4 (132)	50 (191)	320 (184)	670 (209)	29 (183)

[a]Rates [Can^r x 10^{-7}] for particular types of mutations were calculated as described previously (24);
[b]Number of events for specific classes of mutations are shown in brackets;
[c]Indels include minus and plus one nucleotide mutations;
[d]TBPS are tandem base pair substitutions;
[e]Complex mutations are defined as multiple changes within short DNA stretches (separated by up to 10 nt).
5% or less of sequenced Can^r yeast colonies were wild type and they were not included in the analysis.

experiments. First, we partially inactivated MMR by deleting the *MSH6* gene from the *pol2-16 rev3Δ* strain. *MSH6* is a component of MutSα, the heterodimer that initiates the correction of base•base mismatches and small indel loops made by Pols α, δ and ε (14,39), but not mismatches made by Pol ζ (40,41). Consistent with previous reports (42), the mutation rate in the *msh6Δ* strain was 40 × 10^{-7} (Table 1), representing a 10-fold increase over the rate in wild type cells ($P < 0.0001$, Supplementary Data 1). Also consistent with other studies indicating that Pol ζ-dependent mutagenesis is independent of MMR (40,43), the mutation rate was largely unaffected by also deleting *REV3* (*msh6Δ rev3Δ,* 49 × 10^{-7}, Table 1). However, the mutation rate in the *pol2-16 rev3Δ msh6Δ* triple mutant strain is 320 × 10^{-7} (Table 1). This large increase in rate when Msh6 is missing is consistent with robust MMR of replication errors created in the *pol2-16 rev3Δ* mutant ($P < 0.0001$, Supplementary Data 1).

Evidence that mutations in *pol2-16 rev3Δ* are generated by Pol δ

Sequence analysis of Can^r yeast colonies from *pol2-16 rev3Δ* versus *pol2-16 rev3Δ msh6Δ* strains (Table 2, Figure 3A and Supplementary Table S1) reveals that loss of Msh6-dependent MMR largely increases rates for the three base substitutions that are most commonly created by Pol δ (30), namely A•T to G•C transitions via template T•dGMP mismatches, G•C to A•T transitions via template G•dTMP mismatches, and G•C to T•A transversions via template C•dTMP mismatches (Figure 3A; for all three mutation types $P \leq 0.0001$, Supplementary Data 1). These data are consistent with our previous interpretation based on HydEn-seq analysis that Pol δ is the primary replicase for both DNA strands in the *pol2-16* mutant (22).

As a further test of this hypothesis, we compared mutation rates and specificity in strains encoding a mutator allele

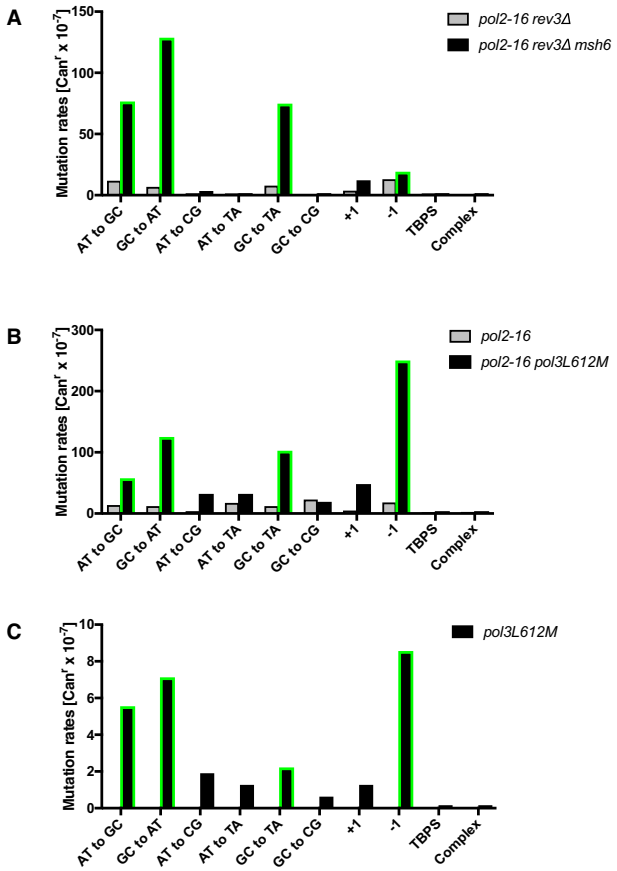

Figure 3. Pol δ is responsible for a fraction of mutations in the *pol2-16* mutant. Data in diagrams **A**–**C** are from Table 2 and show the mutation rates of specific mutation classes measured for *pol2-16 rev3Δ*, *pol2-16 rev3Δ msh6Δ* (panel A), *pol2-16*, *pol2-16 pol3L612M* (panel B) and *pol3L612M* yeast (panel C). Grey and black bars represent different genotypes. Green borderline of bars indicates mutation classes characteristic for L612M Pol δ.

of Pol δ, *pol3L612M*. Strains harboring this mutator allele generate Pol δ-dependent replication errors at an increased rate (14,30), as exemplified here by the 7-fold increase in mutation rate of the *pol3L612M* mutant compared to the wild type strain (Table 1). In this strain background, the addition of the *pol2-16* mutation increases the mutation rate to 670 $\times 10^{-7}$ ($P < 0.0001$, Supplementary Data 1), representing a 160-fold increase over the rate in the wild type strain. Moreover, the *CAN1* mutation spectrum (Table 2 and Supplementary Table S1) reveals that this strong increase is largely due to increases in the same three base-base mismatches mentioned immediately above (for all three mutation types $P < 0.0001$, Supplementary Data 1), plus single-base deletions ($P < 0.0001$, Supplementary Data 1) that are also characteristic of replication errors generated by L612M Pol δ (Figure 3C and (14,30)).

To further examine the role of Pol δ in replication of both DNA strands in the *pol2-16* mutant, we next performed a pairwise comparisons of the *CAN1* mutation spectra quantified in Figure 4 and Supplementary Table S1. Both wild type and L612M Pol δ have established preferences for T•dGMP over complementary A•dCMP mismatches (30). Given that *CAN1* is replicated by forks originating from *ARS507* roughly 98% of the time (15), we can infer the coding strand of *CAN1* is usually the template for lagging strand synthesis. If Pol δ replicates only one strand (Figure 4A-left panel), then we expect a high ratio of T to C versus A to G substitutions at *CAN1* (Figure 4A, left panel). If Pol δ replicates both strands we would expect a ratio closer to 1 (how close depends on details of sequence specificity and whether the Pol δ mutation rate would be the same on both strands; Figure 4A, right panel). In the *pol3L612M* strain, the ratio of T to C versus A to G substitutions is 33.7 (Figure 4B-left panel). However, the ratio drops to only 2.6 in the *pol2-16 pol3L612M* double mutant that lacks Pol ε catalytic activities ($P = 0.002$, Supplementary Data 1). A similar result is seen for G to A versus C to T substitutions in the latter two strains, where the ratio drops from 13.9 to 3.3 (Figure 4C; $P = 0.02$, Supplementary Data 1). In the *rev3Δ msh6Δ* strain, the ratio of G to A versus C to T substitutions is 7.6 (Figure 4D-left panel). However, the ratio drops to only 1.6 in the *pol2-16 rev3Δ msh6Δ* triple mutant that lacks Pol ε catalytic activities ($P \leq 0.001$, Supplementary Data 1). These data are consistent with the interpretation that Pol δ is the major replicase for one DNA strand in wild type cells and both strands when the catalytic activities of Pol ε are missing.

In wild type yeast at the *CAN1* locus Pol δ synthesizes the majority of the lagging strand while Pol ε works predominantly on the leading strand. Replacement of the wild type Pol δ with the *pol3L612M* variant results in a seven-fold increase in mutation rate as compared to wild type yeast (29 $\times 10^{-7}$ in the *po3L612M* vs 4 $\times 10^{-7}$ for wild type; Table 1). When we remove the Pol ε catalytic domains in the *pol2-16 pol3L612M* double mutant, we observe a multiplicative increase in the mutation rates as compared to single mutants (from 29 $\times 10^{-7}$ for *pol3L612M* and 110 $\times 10^{-7}$ for the *pol2-16* to 670 $\times 10^{-7}$ in *pol2-16 pol3L612M*; Table 1). These results suggest that there are additional factors affecting the fidelity of DNA synthesis due to lack of Pol ε's catalytic domains (*pol2-16*). The effect could reflect the dNTP pool increases observed in the *pol2-16* yeast, which is known to be a very important determinant of the fidelity of DNA polymerases (28,44–48).

DISCUSSION

The results presented here are consistent with the following interpretations regarding the fidelity of nuclear DNA replication when the catalytic activities of Pol ε are missing.

As we and others have shown earlier, the lack of Pol ε's catalytic domains causes impaired cell cycle progression and an elongated S-phase, and it significantly enlarges the size of the cell and the nucleus (22,49,50). Here we show that the *pol2-16* mutant also has a significantly decreased level of Sml1, a ribonucleotide reductase (RNR) inhibitor, and increased dNTP levels (Figure 1). All of these phenotypes suggest that lack of Pol ε's catalytic domains leads to a replication stress and S-phase checkpoint activation. Such replication stress and accompanying increased dNTPs pool are associated with genome instability and increased spontaneous mutation rates (51–56).

Previous studies by Sugino *et al.* (49) indicated that the *pol2-16* mutant has mutation rates that are only slightly greater than wild type, e.g., by only 1.6-fold at the *URA3* locus. This contrasts with our results demonstrating that *pol2-16* is a much more robust mutator, with a mutation rate at *CAN1* that is 27-fold higher than for wild type cells and even higher than that of a MMR defective strain (Table 1). The difference between our measurements and those reported earlier is potentially explained by the rapid accumulation of suppressors acquired by the *pol2-16* mutant (22). The nature of the suppression is under investigation. To minimize selection of suppressors that affect growth (22) and may affect mutagenesis, in all experiments we used *pol2-16* spore colonies from a freshly dissected heterozygous diploid *pol2-16/POL2*. The strong increase in mutation rate in the *pol2-16* mutant cannot be explained simply by loss of Pol ε proofreading activity, because inactivation of this activity in the *pol2-4* mutant leads only to a moderate increase in mutation rate ((4,25,41) and Table 1), and does so without increasing dNTP pools (55). In addition, while Pol ε proofreads its own mismatches, it may not proofread mismatches made by Pol α (57) and possibly Pol δ (58).

In agreement with results published earlier (32,33), *REV3* deletion in otherwise wild type yeast causes an ∼2-fold decrease in the spontaneous mutation rate (Table 1). A similar decrease is conferred in the *pol2-16* mutant upon *REV3* deletion. The mutations that disappear (colored pink in Figure 2) are those reported to be generated by Pol ζ, namely complex mutations and transversions. We previously proposed that complex mutations, which contain two or more single base substitutions and indels within about 10 base pairs of each other, are generated by Pol ζ during short stretches of processive DNA synthesis (59). The substitutions include A•T to C•G, A•T to T•A and G•C to C•G transversions (Figure 2C and D). All four classes of mutations are hallmarks of error-prone DNA synthesis by Pol ζ (25,33–35,37,38,41,60–62). In particular, the complex mutations and GC to CG transversions have been suggested to occur when replication stalls due to presence of atypical DNA structures, such as hairpins or non-B-form DNA

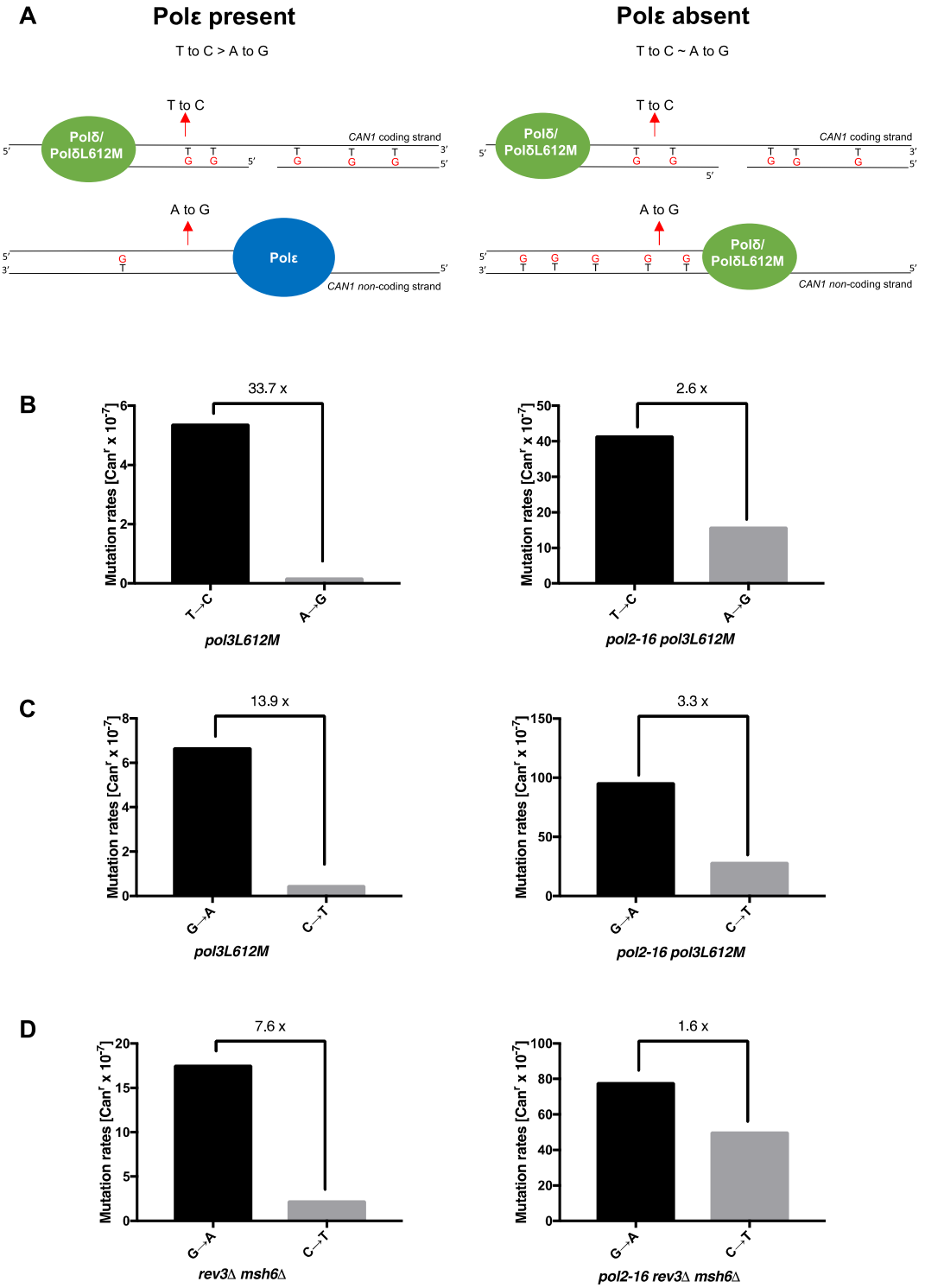

Figure 4. Mutation rates of specific events (reciprocal mistakes). Panel **A** represent a model of what is expected if Pol δ does only lagging strand synthesis (left) as opposed to the synthesis of both leading and lagging strands (right). Panels **B**–**D** represent the mutation rate [Can^r x 10^{-7}] for a specific event types. See text for explanations. A full list of all detected events for *pol3L612M, pol2-16 pol3L612M, rev3Δ msh6Δ* and *pol2-16 rev3Δ msh6Δ* strains is presented in Supplementary Table S1.

structures (6). Under normal conditions Pol ε is physically connected to the moving fork via the CMG helicase (63,64), but when Pol ε catalytic domains are absent (*pol2-16*), Pol δ, which is excluded from the CMG (65), becomes the leading strand replicase. This physical uncoupling of unwinding (2) and leading strand synthesis may allow ssDNA secondary structure formation and thus an increase in mutagenic synthesis by Pol ζ. By extrapolation, this implies that under circumstances when Pol ε is fully active, Pol ζ will contribute less to mutagenic synthesis of genomic DNA.

The synergistic increase in mutation rates in the *pol2-16 rev3Δ msh6Δ* mutant as compared to those in the *pol2-16 rev3Δ* and *rev3Δ msh6Δ* mutants reveals that the errors made in the *pol2-16 rev3Δ* mutant strain are substrate for MMR, indicating that they are generated during DNA replication. Moreover, the mutational specificity (green bars in Figure 3A) is consistent with mutations made by Pol δ. These include the two transitions, A•T to G•C and G•C to A•T, the G•C to T•A transversions and also indel mutations, as seen in previous studies (14,30) and as observed here in the *pol2-16 pol3-L612M* strain (Figure 3B). The high rates at which all these mutations are generated are also consistent with the high dNTP concentrations observed in the *pol2-16* background.

The L686M variant of Pol δ extends mismatches more efficiently as compared to wild type Pol δ and therefore proofreads mismatches less efficiently, despite retaining normal 3′ exonuclease activity (30). In the *pol2-16* mutant studied here, dNTP pools are increased, and the same classes of base substitution mutations are observed as those in the *pol3L686M* mutant (Figure 3B and C). These facts suggest that the mutator effect in the *pol2-16* mutant partly reflects impaired proofreading by Pol δ that is caused by the higher concentration of dNTPs. This interpretation is consistent with data *in vitro* demonstrating that proofreading is suppressed as the concentration of the next correct dNTP is increased (28,66,67).

Analysis of reciprocal mutation classes using polymerase variants have been used to assign DNA polymerases to specific DNA strands (13,14,23) and (Figure 4A). Here, we analyzed the specificity of mutations in strains with and without Pol ε's catalytic subunit (*POL2* and *pol2-16,* respectively), as well as bearing either the wild type or a mutator variant of Pol δ (*POL3* and *pol3L612M*, respectively). Studies of the *pol3L612M* mutant *in vitro* have previously demonstrated that this variant of Pol δ incorporates dG opposite T in the template about 28-fold more frequently than it incorporates the complementary dC opposite A in the template (30). This fact, coupled with the fact that the coding strand of *CAN1* is the template for lagging strand synthesis, predicts more T to C mutations than A to G mutations in the *pol3L612M* yeast, where Pol δ predominantly synthesizes the lagging strand (Figure 4). By analyzing the ratio of T to C versus A to G, we can determine whether Pol δ works on one (Figure 4A, left panel) or both DNA strands (Figure 4A, right panel). The ratio of T to C versus A to G mutations was 33.7 in the *pol3L612M* (Figure 4B, left panel) and decreased to only 2.6 in the *pol2-16 pol3L612M* (Figure 4B, right panel), indicating that both strands are synthesized by Pol δ. Similarly, the ratio of G to A vs C to T was 13.9 in the *pol3L612M* strain (Figure 4C, left panel) and decreased to only 3.3 in the *pol2-16 pol3L612M* (Figure 4C, right panel). Moreover, whole genome mutation accumulation experiments in yeast strains bearing the *pol3L612M* variant of Pol δ reveal that the rates of A to G vs T to C and of G to A vs C to T mutations are also biased when MMR is active (14). In the present study, the ratio of G to A vs C to T dropped from 7.6 in the *rev3Δ msh6Δ* strain to 1.6 (Figure 4D, left panel) in the *pol2-16 rev3Δ msh6Δ* triple mutant (Figure 4D, right panel). The stronger mutational biases in the strain with Pol ε catalytic activity than in the *pol2-16* mutant strain without Pol ε catalytic domains are also consistent with previous HydEn-seq results showing Pol δ synthesis of both leading and lagging DNA strands when Pol ε catalytic domains are not present (22).

Here we present an extreme case wherein Pol δ is the major replicase for both the leading strand and the lagging strand across the entire genome due to lack of catalytic domains of Pol ε. This situation is likely to be relevant even in cells with wild type Pol ε. This is because in some circumstances, Pol δ has been shown to synthesize both the leading and lagging strands in a more local manner, for example during break-induced replication (68,69) and during homologous recombination-dependent replication fork restart (70). Both of these processes are mutagenic.

The catalytic subunit of Pol ε is composed of an amino terminal region possessing its two catalytic activities, and a carboxy-terminal region involved in checkpoint control (71–73). Both regions of Pol ε are involved in a network of interactions with other components of the replisome. For example, crosslinking mass spectrometry analysis identified Pol2p interactors that include Cdc45, Psf1, Mcm2, Mcm 5 and Mcm6 (74,75). Lack of the N-terminal lobe of Pol2p in the *pol2-16* mutant may disturb interactions with other components of the replisome affecting both the replication initiation as well as DNA replication progression, thereby allowing other DNA polymerases to have access to the primer terminus more frequently.

SUPPLEMENTARY DATA

Supplementary Data are available at NAR Online.

ACKNOWLEDGEMENTS

We thank Kasia Bebenek and Roel Schaaper for critical reading of and thoughtful comments on the manuscript. We thank all members of the DNA replication fidelity group for helpful discussions throughout the work. We are grateful to Dmitry Gordenin for providing the source of *rev3Δ::KanMX4* cassette.

FUNDING

Division of Intramural Research of the NIH [Z01 ES065070 to T.A.K.]; NIEHS; Swedish Cancer Society and the Swedish Research Council (to A.C.). Funding for open access charge: Division of Intramural Research of the NIH, NIEHS [Z01 ES065070 to T.A.K.].
Conflict of interest statement. None declared.

REFERENCES

1. Stillman,B. (2015) Reconsidering DNA polymerases at the replication fork in eukaryotes. *Mol. Cell*, **59**, 139–141.
2. Yeeles,J.T., Janska,A., Early,A. and Diffley,J.F. (2017) How the eukaryotic replisome achieves rapid and efficient DNA replication. *Mol. Cell*, **65**, 105–116.
3. Schauer,G.D. and O'Donnell,M.E. (2017) Quality control mechanisms exclude incorrect polymerases from the eukaryotic replication fork. *Proc. Natl. Acad. Sci. U.S.A.*, **114**, 675–680.
4. Georgescu,R., Yuan,Z., Bai,L., de Luna Almeida Santos,R., Sun,J., Zhang,D., Yurieva,O., Li,H. and O'Donnell,M.E. (2017) Structure of eukaryotic CMG helicase at a replication fork and implications to replisome architecture and origin initiation. *Proc. Natl. Acad. Sci. U.S.A.*, **114**, E697–E706.
5. Makarova,A.V. and Burgers,P.M. (2015) Eukaryotic DNA polymerase zeta. *DNA Repair (Amst.)*, **29**, 47–55.
6. Northam,M.R., Moore,E.A., Mertz,T.M., Binz,S.K., Stith,C.M., Stepchenkova,E.I., Wendt,K.L., Burgers,P.M. and Shcherbakova,P.V. (2014) DNA polymerases zeta and Rev1 mediate error-prone bypass of non-B DNA structures. *Nucleic Acids Res.*, **42**, 290–306.
7. Shcherbakova,P.V., Pavlov,Y.I., Chilkova,O., Rogozin,I.B., Johansson,E. and Kunkel,T.A. (2003) Unique error signature of the four-subunit yeast DNA polymerase epsilon. *J. Biol. Chem.*, **278**, 43770–43780.
8. Fortune,J.M., Pavlov,Y.I., Welch,C.M., Johansson,E., Burgers,P.M. and Kunkel,T.A. (2005) Saccharomyces cerevisiae DNA polymerase delta: high fidelity for base substitutions but lower fidelity for single- and multi-base deletions. *J. Biol. Chem.*, **280**, 29980–29987.
9. Burgers,P.M.J. and Kunkel,T.A. (2017) Eukaryotic DNA replication fork. *Annu. Rev. Biochem.*, **86**, 417–438.
10. Kunkel,T.A. and Burgers,P.M.J. (2017) Arranging eukaryotic nuclear DNA polymerases for replication: Specific interactions with accessory proteins arrange Pols alpha, delta, and in the replisome for leading-strand and lagging-strand DNA replication. *Bioessays*, **39**, doi:10.1002/bies.201700070.
11. Lujan,S.A., Williams,J.S. and Kunkel,T.A. (2016) DNA polymerases divide the labor of genome replication. *Trends Cell Biol.*, **26**, 640–654.
12. Johnson,R.E., Klassen,R., Prakash,L. and Prakash,S. (2015) A major role of DNA polymerase δ in replication of both the leading and lagging DNA strands. *Mol. Cell*, **59**, 163–175.
13. Pursell,Z.F., Isoz,I., Lundstrom,E.B., Johansson,E. and Kunkel,T.A. (2007) Yeast DNA polymerase epsilon participates in leading-strand DNA replication. *Science*, **317**, 127–130.
14. Lujan,S.A., Clausen,A.R., Clark,A.B., MacAlpine,H.K., MacAlpine,D.M., Malc,E.P., Burkholder,A.B., Fargo,D.C., Gordenin,D.A. and Kunkel,T.A. (2014) Heterogeneous polymerase fidelity and mismatch repair bias genome variation and composition. *Genome Res.*, **24**, 1751–1764.
15. Clausen,A.R., Lujan,S.A., Burkholder,A.B., Orebaugh,C.D., Williams,J.S., Clausen,M.F., Malc,E.P., Mieczkowski,P.A., Fargo,D.C., Smith,D.J. *et al.* (2015) Tracking replication enzymology in vivo by genome-wide mapping of ribonucleotide incorporation. *Nat. Struct. Mol. Biol.*, **22**, 185–191.
16. Daigaku,Y., Keszthelyi,A., Muller,C.A., Miyabe,I., Brooks,T., Retkute,R., Hubank,M., Nieduszynski,C.A. and Carr,A.M. (2015) A global profile of replicative polymerase usage. *Nat Struct Mol Biol*, **22**, 192–198.
17. Williams,J.S., Lujan,S.A. and Kunkel,T.A. (2016) Processing ribonucleotides incorporated during eukaryotic DNA replication. *Nat. Rev. Mol. Cell Biol.*, **17**, 350–363.
18. Koh,K.D., Balachander,S., Hesselberth,J.R. and Storici,F. (2015) Ribose-seq: global mapping of ribonucleotides embedded in genomic DNA. *Nat. Methods*, **12**, 251–257.
19. Langston,L.D., Zhang,D., Yurieva,O., Georgescu,R.E., Finkelstein,J., Yao,N.Y., Indiani,C. and O'Donnell,M.E. (2014) CMG helicase and DNA polymerase epsilon form a functional 15-subunit holoenzyme for eukaryotic leading-strand DNA replication. *Proc. Natl. Acad. Sci. U.S.A.*, **111**, 15390–15395.
20. Shinbrot,E., Henninger,E.E., Weinhold,N., Covington,K.R., Goksenin,A.Y., Schultz,N., Chao,H., Doddapaneni,H., Muzny,D.M., Gibbs,R.A. *et al.* (2014) Exonuclease mutations in DNA polymerase epsilon reveal replication strand specific mutation patterns and human origins of replication. *Genome Res.*, **24**, 1740–1750.
21. Haradhvala,N.J., Polak,P., Stojanov,P., Covington,K.R., Shinbrot,E., Hess,J.M., Rheinbay,E., Kim,J., Maruvka,Y.E., Braunstein,L.Z. *et al.* (2016) Mutational strand asymmetries in cancer genomes reveal mechanisms of DNA damage and repair. *Cell*, **164**, 538–549.
22. Garbacz,M.A., Lujan,S.A., Burkholder,A.B., Cox,P.B., Wu,Q., Zhou,Z.X., Haber,J.E. and Kunkel,T.A. (2018) Evidence that DNA polymerase delta contributes to initiating leading strand DNA replication in Saccharomyces cerevisiae. *Nat. Commun.*, **9**, 858.
23. Nick McElhinny,S.A., Gordenin,D.A., Stith,C.M., Burgers,P.M. and Kunkel,T.A. (2008) Division of labor incorporation into DNA at the eukaryotic replication fork. *Moll Cell*, **30**, 137–144.
24. Lujan,S.A., Williams,J.S., Pursell,Z.F., Abdulovic-Cui,A.A., Clark,A.B., McElhinny,S.A.N. and Kunkel,T.A. (2012) Mismatch repair balances leading and lagging strand DNA replication fidelity. *PLoS Genet.*, **8**, e1003016.
25. Garbacz,M., Araki,H., Flis,K., Bebenek,A., Zawada,A.E., Jonczyk,P., Makiela-Dzbenska,K. and Fijalkowska,I.J. (2015) Fidelity consequences of the impaired interaction between DNA polymerase epsilon and the GINS complex. *DNA Repair (Amst.)*, **29**, 23–35.
26. Lujan,S.A., Williams,J.S., Clausen,A.R., Clark,A.B. and Kunkel,T.A. (2013) Ribonucleotides are signals for mismatch repair of leading-strand replication errors. *Mol. Cell*, **50**, 437–443.
27. Zbyněk,Š. (1967) Rectangular confidence regions for the means of multivariate normal distributions. *J. Am. Stat. Assoc.*, **62**, 626–633.
28. Watt,D.L., Buckland,R.J., Lujan,S.A., Kunkel,T.A. and Chabes,A. (2016) Genome-wide analysis of the specificity and mechanisms of replication infidelity driven by imbalanced dNTP pools. *Nucleic Acids Res.*, **44**, 1669–1680.
29. Sabouri,N., Viberg,J., Goyal,D.K., Johansson,E. and Chabes,A. (2008) Evidence for lesion bypass by yeast replicative DNA polymerases during DNA damage. *Nucleic Acids Res.*, **36**, 5660–5667.
30. Nick McElhinny,S.A., Stith,C.M., Burgers,P.M. and Kunkel,T.A. (2007) Inefficient proofreading and biased error rates during inaccurate DNA synthesis by a mutant derivative of Saccharomyces cerevisiae DNA polymerase delta. *J. Biol. Chem.*, **282**, 2324–2332.
31. Stone,J.E., Lujan,S.A., Kunkel,T.A. and Kunkel,T.A. (2012) DNA polymerase zeta generates clustered mutations during bypass of endogenous DNA lesions in Saccharomyces cerevisiae. *Environ. Mol. Mutagen.*, **53**, 777–786.
32. Northam,M.R., Garg,P., Baitin,D.M., Burgers,P.M. and Shcherbakova,P.V. (2006) A novel function of DNA polymerase zeta regulated by PCNA. *EMBO J.*, **25**, 4316–4325.
33. Northam,M.R., Robinson,H.A., Kochenova,O.V. and Shcherbakova,P.V. (2010) Participation of DNA polymerase zeta in replication of undamaged DNA in Saccharomyces cerevisiae. *Genetics*, **184**, 27–42.
34. Zhong,X., Garg,P., Stith,C.M., Nick McElhinny,S.A., Kissling,G.E., Burgers,P.M. and Kunkel,T.A. (2006) The fidelity of DNA synthesis by yeast DNA polymerase zeta alone and with accessory proteins. *Nucleic Acids Res.*, **34**, 4731–4742.
35. Kochenova,O.V., Bezalel-Buch,R., Tran,P., Makarova,A.V., Chabes,A., Burgers,P.M. and Shcherbakova,P.V. (2017) Yeast DNA polymerase zeta maintains consistent activity and mutagenicity across a wide range of physiological dNTP concentrations. *Nucleic Acids Res.*, **45**, 1200–1218.
36. Roche,H., Gietz,R.D. and Kunz,B.A. (1994) Specificity of the yeast Rev3-Delta antimutator and Rev3 dependency of the mutator resulting from a defect (Rad1-Delta) in nucleotide Excision-Repair. *Genetics*, **137**, 637–646.
37. Kraszewska,J., Garbacz,M., Jonczyk,P., Fijalkowska,I.J. and Jaszczur,M. (2012) Defect of Dpb2p, a noncatalytic subunit of DNA polymerase varepsilon, promotes error prone replication of undamaged chromosomal DNA in Saccharomyces cerevisiae. *Mutat. Res.*, **737**, 34–42.
38. Szwajczak,E., Fijalkowska,I.J. and Suski,C. (2017) The CysB motif of Rev3p involved in the formation of the four-subunit DNA polymerase zeta is required for defective-replisome-induced mutagenesis. *Mol. Microbiol.*, **106**, 659–672.
39. Marsischky,G.T., Filosi,N., Kane,M.F. and Kolodner,R. (1996) Redundancy of Saccharomyces cerevisiae MSH3 and MSH6 in MSH2-dependent mismatch repair. *Genes Dev.*, **10**, 407–420.

40. Huang,M.E., Rio,A.G., Galibert,M.D. and Galibert,F. (2002) Pol32, a subunit of Saccharomyces cerevisiae DNA polymerase delta, suppresses genomic deletions and is involved in the mutagenic bypass pathway. *Genetics*, **160**, 1409–1422.
41. Aksenova,A., Volkov,K., Maceluch,J., Pursell,Z.F., Rogozin,I.B., Kunkel,T.A., Pavlov,Y.I. and Johansson,E. (2010) Mismatch repair-independent increase in spontaneous mutagenesis in yeast lacking non-essential subunits of DNA polymerase epsilon. *PLoS Genet.*, **6**, e1001209.
42. Flores-Rozas,H. and Kolodner,R.D. (1998) The Saccharomyces cerevisiae MLH3 gene functions in MSH3-dependent suppression of frameshift mutations. *Proc. Natl. Acad. Sci. U.S.A.*, **95**, 12404–12409.
43. Lehner,K. and Jinks-Robertson,S. (2009) The mismatch repair system promotes DNA polymerase zeta-dependent translesion synthesis in yeast. *Proc. Natl. Acad. Sci. U.S.A.*, **106**, 5749–5754.
44. Chabes,A., Georgieva,B., Domkin,V., Zhao,X., Rothstein,R. and Thelander,L. (2003) Survival of DNA damage in yeast directly depends on increased dNTP levels allowed by relaxed feedback inhibition of ribonucleotide reductase. *Cell*, **112**, 391–401.
45. Kumar,D., Viberg,J., Nilsson,A.K. and Chabes,A. (2010) Highly mutagenic and severely imbalanced dNTP pools can escape detection by the S-phase checkpoint. *Nucleic Acids Res.*, **38**, 3975–3983.
46. Kumar,D., Abdulovic,A.L., Viberg,J., Nilsson,A.K., Kunkel,T.A. and Chabes,A. (2011) Mechanisms of mutagenesis in vivo due to imbalanced dNTP pools. *Nucleic Acids Res.*, **39**, 1360–1371.
47. Mertz,T.M., Sharma,S., Chabes,A. and Shcherbakova,P.V. (2015) Colon cancer-associated mutator DNA polymerase delta variant causes expansion of dNTP pools increasing its own infidelity. *Proc. Natl. Acad. Sci. U.S.A.*, **112**, E2467–E2476.
48. Bebenek,K., Roberts,J.D. and Kunkel,T.A. (1992) The effects of dNTP pool imbalances on frameshift fidelity during DNA replication. *J. Biol. Chem.*, **267**, 3589–3596.
49. Ohya,T., Kawasaki,Y., Hiraga,S., Kanbara,S., Nakajo,K., Nakashima,N., Suzuki,A. and Sugino,A. (2002) The DNA polymerase domain of pol(epsilon) is required for rapid, efficient, and highly accurate chromosomal DNA replication, telomere length maintenance, and normal cell senescence in Saccharomyces cerevisiae. *J. Biol. Chem.*, **277**, 28099–28108.
50. Kesti,T., Flick,K., Keranen,S., Syvaoja,J.E. and Wittenberg,C. (1999) DNA polymerase epsilon catalytic domains are dispensable for DNA replication, DNA repair, and cell viability. *Mol. Cell*, **3**, 679–685.
51. Davidson,M.B., Katou,Y., Keszthelyi,A., Sing,T.L., Xia,T., Ou,J., Vaisica,J.A., Thevakumaran,N., Marjavaara,L., Myers,C.L. *et al.* (2012) Endogenous DNA replication stress results in expansion of dNTP pools and a mutator phenotype. *EMBO J.*, **31**, 895–907.
52. Williams,J.S., Clausen,A.R., Nick McElhinny,S.A., Watts,B.E., Johansson,E. and Kunkel,T.A. (2012) Proofreading of ribonucleotides inserted into DNA by yeast DNA polymerase epsilon. *DNA Repair (Amst.)*, **11**, 649–656.
53. Chabes,A. and Stillman,B. (2007) Constitutively high dNTP concentration inhibits cell cycle progression and the DNA damage checkpoint in yeast Saccharomyces cerevisiae. *Proc. Natl. Acad. Sci. U.S.A.*, **104**, 1183–1188.
54. Kumar,D., Abdulovic,A.L., Viberg,J., Nilsson,A.K., Kunkel,T.A. and Chabes,A. (2011) Mechanisms of mutagenesis in vivo due to imbalanced dNTP pools. *Nucleic Acids Res.*, **39**, 1360–1371.
55. Williams,L.N., Marjavaara,L., Knowels,G.M., Schultz,E.M., Fox,E.J., Chabes,A. and Herr,A.J. (2015) dNTP pool levels modulate mutator phenotypes of error-prone DNA polymerase epsilon variants. *Proc. Natl. Acad. Sci. U.S.A.*, **112**, E2457–E2466.
56. Mertz,T.M., Sharma,S., Chabes,A. and Shcherbakova,P.V. (2015) Colon cancer-associated mutator DNA polymerase delta variant causes expansion of dNTP pools increasing its own infidelity. *Proc. Natl. Acad. Sci. U.S.A.*, **112**, E2467–E2476.
57. Pavlov,Y.I., Frahm,C., Nick McElhinny,S.A., Niimi,A., Suzuki,M. and Kunkel,T.A. (2006) Evidence that errors made by DNA polymerase alpha are corrected by DNA polymerase delta. *Curr. Biol.*, **16**, 202–207.
58. Flood,C.L., Rodriguez,G.P., Bao,G., Shockley,A.H., Kow,Y.W. and Crouse,G.F. (2015) Replicative DNA polymerase delta but not epsilon proofreads errors in Cis and in Trans. *PLoS Genet.*, **11**, e1005049.
59. Stone,J.E., Kissling,G.E., Lujan,S.A., Rogozin,I.B., Stith,C.M., Burgers,P.M. and Kunkel,T.A. (2009) Low-fidelity DNA synthesis by the L979F mutator derivative of Saccharomyces cerevisiae DNA polymerase zeta. *Nucleic Acids Res.*, **37**, 3774–3787.
60. Pavlov,Y.I., Shcherbakova,P.V. and Kunkel,T.A. (2001) In vivo consequences of putative active site mutations in yeast DNA polymerases alpha, epsilon, delta, and zeta. *Genetics*, **159**, 47–64.
61. Shcherbakova,P.V. and Fijalkowska,I.J. (2006) Translesion synthesis DNA polymerases and control of genome stability. *Front. Biosci.*, **11**, 2496–2517.
62. Zheng,D.Q., Zhang,K., Wu,X.C., Mieczkowski,P.A. and Petes,T.D. (2016) Global analysis of genomic instability caused by DNA replication stress in Saccharomyces cerevisiae. *Proc. Natl. Acad. Sci. U.S.A.*, **113**, E8114–E8121.
63. Sengupta,S., van Deursen,F., de Piccoli,G. and Labib,K. (2013) Dpb2 integrates the leading-strand DNA polymerase into the eukaryotic replisome. *Curr. Biol.*, **23**, 543–552.
64. Muramatsu,S., Hirai,K., Tak,Y.S., Kamimura,Y. and Araki,H. (2010) CDK-dependent complex formation between replication proteins Dpb11, Sld2, Pol (epsilon}, and GINS in budding yeast. *Genes Dev.*, **24**, 602–612.
65. Georgescu,R.E., Schauer,G.D., Yao,N.Y., Langston,L.D., Yurieva,O., Zhang,D., Finkelstein,J. and O'Donnell,M.E. (2015) Reconstitution of a eukaryotic replisome reveals suppression mechanisms that define leading/lagging strand operation. *Elife*, **4**, e04988.
66. Creighton,S. and Goodman,M.F. (1995) Gel kinetic analysis of DNA polymerase fidelity in the presence of proofreading using bacteriophage T4 DNA polymerase. *J. Biol. Chem.*, **270**, 4759–4774.
67. Beckman,R.A. and Loeb,L.A. (1993) Multi-stage proofreading in DNA replication. *Q. Rev. Biophys.*, **26**, 225–331.
68. Deem,A., Keszthelyi,A., Blackgrove,T., Vayl,A., Coffey,B., Mathur,R., Chabes,A. and Malkova,A. (2011) Break-induced replication is highly inaccurate. *PLoS Biol.*, **9**, e1000594.
69. Lydeard,J.R., Jain,S., Yamaguchi,M. and Haber,J.E. (2007) Break-induced replication and telomerase-independent telomere maintenance require Pol32. *Nature*, **448**, 820–823.
70. Miyabe,I., Mizuno,K., Keszthelyi,A., Daigaku,Y., Skouteri,M., Mohebi,S., Kunkel,T.A., Murray,J.M. and Carr,A.M. (2015) Polymerase delta replicates both strands after homologous recombination-dependent fork restart. *Nat. Struct. Mol. Biol.*, **22**, 932–938.
71. Dua,R., Levy,D.L. and Campbell,J.L. (1999) Analysis of the essential functions of the C-terminal protein/protein interaction domain of *Saccharomyces cerevisiae* pol e and its unexpected ability to support growth in the absence of the DNA polymerase domain. *J. Biol. Chem.*, **274**, 22283–22288.
72. Goswami,P., Abid Ali,F., Douglas,M.E., Locke,J., Purkiss,A., Janska,A., Eickhoff,P., Early,A., Nans,A., Cheung,A.M.C. *et al.* (2018) Structure of DNA-CMG-Pol epsilon elucidates the roles of the non-catalytic polymerase modules in the eukaryotic replisome. *Nat. Commun.*, **9**, 5061.
73. Tahirov,T.H., Makarova,K.S., Rogozin,I.B., Pavlov,Y.I. and Koonin,E.V. (2009) Evolution of DNA polymerases: an inactivated polymerase-exonuclease module in Pol epsilon and a chimeric origin of eukaryotic polymerases from two classes of archaeal ancestors. *Biol. Direct*, **4**, 11.
74. Sun,J., Shi,Y., Georgescu,R.E., Yuan,Z., Chait,B.T., Li,H. and O'Donnell,M.E. (2015) The architecture of a eukaryotic replisome. *Nat. Struct. Mol. Biol.*, **22**, 976–982.
75. Yuan,Z., Bai,L., Sun,J., Georgescu,R., Liu,J., O'Donnell,M.E. and Li,H. (2016) Structure of the eukaryotic replicative CMG helicase suggests a pumpjack motion for translocation. *Nat. Struct. Mol. Biol.*, **23**, 217–224.